arXiv:1106.0558v4 [nlin.CD] 9 Dec 2012

UDC 536.46

Random Noise and Pole-Dynamics in Unstable Front Propagation II

Oleg Kupervasser, Zeev Olami
Department of Chemical Physics
The Weizmann Institute of Science
Rehovot 76100, Israel

December 11, 2012

Abstract

The current paper is a corrected version of our previous paper (Olami et al., PRE **55** (3),(1997)). Similarly to previous version we investigate the problem of flame propagation. This problem is studied as an example of unstable fronts that wrinkle on many scales. The analytic tool of pole expansion in the complex plane is employed to address the interaction of the unstable growth process with random initial conditions and perturbations. We argue that the effect of random noise is immense and that it can never be neglected in sufficiently large systems. We present simulations that lead to scaling laws for the velocity and acceleration of the front as a function of the system size and the level of noise, and analytic arguments that explain these results in terms of the noisy pole dynamics.This version corrects some very critical errors made in (Olami et al., PRE **55** (3),(1997)) and makes more detailed description of excess number of poles in system , number of poles that appear in the system in unit of time, life time of pole. It allows us to understand more correctly dependence of the system parameters on noise than in (Olami et al., PRE **55** (3),(1997))
Keywords: flame propagation, pole dynamics, unstable front, random noise, self-acceleration

1 Introduction

This article considers the very interesting problem of describing the nonlinear stage of development of hydrodynamic instability of the flame. This problem can be considered for 1D (channel propagation) , 2D (cylindrical case) , 3D (spherical case). The direct numerical simulations can be made based on of the NavierStokes equations including chemical kinetics in the form of the Arrhenius law [1]. For 2D and 3D cases we can

see experimentally observable effects [2], [3] of the self-acceleration of the front of a divergent flame, the formation of cellular structure, and other effects.

Much more simple equation for flame front propagation can be obtained [4], [5] . It is Michelson-Sivashinsky approximation model. The Michelson-Sivashinsky model assumes very serious limitations, such as the smallness of the coefficient of gas expansion and, consequently, the potential flow in the combustion products and fresh mixture, weak nonlinearity, the assumptions of the stabilizing effect of the curvature of the flame front and a linear dependence on the curvature of the normal speed, and others. The calculations with a noise term was performed in both one-dimensional and two-dimensional formulations of the problem in our previous papers [6], [7], [8], [9], [10], [11] and recently by Karlin and Sivashinsky [12] , [13] for 1D, 2D and 3D cases.

Interest of this model stems, firstly, from the fact that despite the serious limitations, this model can qualitatively describe the scenario of hydrodynamic instability and, in particular, the self-acceleration of the front of a divergent flame, the formation of a cellular structure, and other effects. Secondary, this nonlinear model has exact solutions which can be constructed on the basis of pole expansions [14], [15], [16], [17]. This pole expansion method got development in the following papers. There was investigated relationships between pole solutions and partial decomposition in Fourier series [18], between the gas flow field and pole solutions [19]. The future development can be found in our previous papers and the correspondent references inside of [6], [7], [8], [9], [10], [11].

It must be mentioned that the simplest 1D case of the flame front propagation is very important. It was the main reason for creation this papers considering in detail the 1D case. Such investigation of this case allows us to understand qualitatively and quantitatively the pole dynamics. This understanding is a basis for the consideration more complex 2D and 3D cases. The our paper [8] clearly demonstrate this fact. The cellular structure, acceleration exponent for 2D case was found on the basis of 1D results.

The future development of our results is gotten in papers [20], [21], [22]. In the very interesting paper [20] the noise term was considered in the poles-like form. The numerical results for 1D case are in a good consistence with the theoretical results of this paper.

This paper is update version of our previous version [6]. In this version we correct some error. For example, we choose incorrect spectrum width of white noise with constant amplitude during changing size of channel L. As result we didn't obtain in [6] saturation of the frame front velocity during increasing L in contradiction with this paper. The second important error connected to number of regimes defined on the "phase diagram" of the system as a function of L and f. Indeed not three but four such regimes exist. The noise influence theory developed in [6] described transition from regime I to regime II and describe only these two regimes. The regime II can not be observed because of numerical noise. The observable regime III can not be explained by the help theory developed in [6]. To make such explanation we calculate numerically and try explain analytically such values as excess number of poles in system , number of poles that appear in the system in unit of time, life time of pole [11]. The developed theory can explain the existence of small dependence parameters of problem on the noise in regime III.

The rest of the paper is organized as follows. We begin by presenting equations of motion and pole-decomposition in the channel geometry(Section 2).Next Section 3 describes acceleration of the flame front, pole dynamics and noise. And finally (Section 4) we give summary and conclusions.

2 Equations of Motion and Pole-decomposition in the Channel Geometry

It is known that planar flames freely propagating through initially motionless homogeneous combustible mixtures are intrinsically unstable. It was reported that such flames develop characteristic structures which include cusps, and that under usual experimental conditions the flame front accelerates as time goes on. A model in $1+1$ dimensions that pertains to the propagation of flame fronts in channels of width $\tilde{L}$ was proposed in [4]. It is written in terms of position $h(x,t)$ of the flame front above the x-axis. After appropriate rescalings it takes the form:

$$\frac{\partial h(x,t)}{\partial t} = \frac{1}{2}\left[\frac{\partial h(x,t)}{\partial x}\right]^2 + \nu\frac{\partial^2 h(x,t)}{\partial x^2} + I\{h(x,t)\} + 1\ . \tag{1}$$

The domain is $0 < x < \tilde{L}$, ν is a parameter and we use periodic boundary conditions. The functional $I[h(x,t)]$ is the Hilbert transform of derivative which is conveniently defined in terms of the spatial Fourier transform

$$h(x,t) = \int_{-\infty}^{\infty} e^{ikx}\hat{h}(k,t)dk \tag{2}$$

$$I[h(k,t)] = |k|\hat{h}(k,t) \tag{3}$$

For the purpose of introducing the pole-decomposition it is convenient to rescale the domain to $0 < \theta < 2\pi$. Performing this rescaling and denoting the resulting quantities with the same notation we have

$$\frac{\partial h(\theta,t)}{\partial t} = \frac{1}{2L^2}\left[\frac{\partial h(\theta,t)}{\partial \theta}\right]^2 + \frac{\nu}{L^2}\frac{\partial^2 h(\theta,t)}{\partial \theta^2}$$
$$+\frac{1}{L}I\{h(\theta,t)\} + 1\ . \tag{4}$$

In this equation $L = \tilde{L}/2\pi$. Next we change variables to $u(\theta,t) \equiv \partial h(\theta,t)/\partial\theta$. We find

$$\frac{\partial u(\theta,t)}{\partial t} = \frac{u(\theta,t)}{L^2}\frac{\partial u(\theta,t)}{\partial \theta} + \frac{\nu}{L^2}\frac{\partial^2 u(\theta,t)}{\partial \theta^2} + \frac{1}{L}I\{u(\theta,t)\}\ . \tag{5}$$

It is well known that the flat front solution of this equation is linearly unstable. The linear spectrum in k-representation is

$$\omega_k = |k|/L - \nu k^2/L^2\ . \tag{6}$$

There exists a typical scale k_{max} which is the last unstable mode

$$k_{max} = \frac{L}{\nu} \ . \tag{7}$$

Nonlinear effects stabilize a new steady-state which is discussed next.

The outstanding feature of the solutions of this equation is the appearance of cusp-like structures in the developing fronts. Therefore a representation in terms of Fourier modes is very inefficient. Rather, it appears very worthwhile to represent such solutions in terms of sums of functions of poles in the complex plane. It will be shown below that the position of the cusp along the front is determined by the real coordinate of the pole, whereas the height of the cusp is in correspondence with the imaginary coordinate. Moreover, it will be seen that the dynamics of the developing front can be usefully described in terms of the dynamics of the poles. Following [7, 14, 15, 17] we expand the solutions $u(\theta, t)$ in functions that depend on N poles whose position $z_j(t) \equiv x_j(t) + iy_j(t)$ in the complex plane is time dependent:

$$\begin{aligned} u(\theta, t) &= \nu \sum_{j=1}^{N} \cot\left[\frac{\theta - z_j(t)}{2}\right] + c.c. \\ &= \nu \sum_{j=1}^{N} \frac{2\sin[\theta - x_j(t)]}{\cosh[y_j(t)] - \cos[\theta - x_j(t)]} \ , \end{aligned} \tag{8}$$

$$h(\theta, t) = 2\nu \sum_{j=1}^{N} \ln\Big[\cosh(y_j(t)) - \cos(\theta - x_j(t))\Big] + C(t) \ . \tag{9}$$

In (9) $C(t)$ is a function of time. The function (9) is a superposition of quasi-cusps (i.e. cusps that are rounded at the tip). The real part of the pole position (i.e. x_j) is the coordinate (in the domain $[0, 2\pi]$) of the maximum of the quasi-cusp, and the imaginary part of the pole position (i.e y_j) is related to the depth of the quasi-cusp. As y_j decreases the depth of the cusp increases. As $y_j \to 0$ the depth diverges to infinity. Conversely, when $y_j \to \infty$ the depth decreases to zero.

The main advantage of this representation is that the propagation and wrinkling of the front can be described via the dynamics of the poles. Substituting (8) in (5) we derive the following ordinary differential equations for the positions of the poles:

$$-L^2 \frac{dz_j}{dt} = \Big[\nu \sum_{k=1, k\neq j}^{2N} \cot\left(\frac{z_j - z_k}{2}\right) + i\frac{L}{2} sign[Im(z_j)]\Big]. \tag{10}$$

We note that in (8), due to the complex conjugation, we have $2N$ poles which are arranged in pairs such that for $j < N$ $z_{j+N} = \bar{z}_j$. In the second sum in (8) each pair of poles contributed one term. In Eq.(10) we again employ $2N$ poles since all of them interact. We can write the pole dynamics in terms of the real and imaginary parts x_j and y_j. Because of the arrangement in pairs it is sufficient to write the equation for either $y_j > 0$ or for $y_j < 0$. We opt for the first. The equations for the positions of the

poles read

$$-L^2\frac{dx_j}{dt} = \nu \sum_{k=1,k\neq j}^{N} \sin(x_j - x_k)\Bigg[[\cosh(y_j - y_k) \tag{11}$$

$$- \cos(x_j - x_k)]^{-1} + [\cosh(y_j + y_k) - \cos(x_j - x_k)]^{-1}\Bigg]$$

$$L^2\frac{dy_j}{dt} = \nu \sum_{k=1,k\neq j}^{N} \Big(\frac{\sinh(y_j - y_k)}{\cosh(y_j - y_k) - \cos(x_j - x_k)}$$

$$+\frac{\sinh(y_j + y_k)}{\cosh(y_j + y_k) - \cos(x_j - x_k)}\Big) + \nu\coth(y_j) - L. \tag{12}$$

We note that if the initial conditions of the differential equation (5) are expandable in a finite number of poles, these equations of motion preserve this number as a function of time. On the other hand, this may be an unstable situation for the partial differential equation, and noise can change the number of poles. This issue will be examined at length in Section 3. We turn now to a discussion of the steady state solution of the equations of the pole-dynamics.

2.1 Qualitative properties of the stationary solution

The steady-state solution of the flame front propagating in channels of width 2π was presented in Ref.[15]. Using these results we can immediately translate the discussion to a channel of width L. The main results are summarized as follows:

1. There is only one stable stationary solution which is geometrically represented by a giant cusp (or equivalently one finger) and analytically by $N(L)$ poles which are aligned on one line parallel to the imaginary axis. The existence of this solution is made clearer with the following remarks.

2. There exists an attraction between the poles along the real line. This is obvious from Eq.(11) in which the sign of dx_j/dt is always determined by $\sin(x_j - x_k)$. The resulting dynamics merges all the x positions of poles whose y-position remains finite.

3. The y positions are distinct, and the poles are aligned above each others in positions $y_{j-1} < y_j < y_{j+1}$ with the maximal being $y_{N(L)}$. This can be understood from Eq.(12) in which the interaction is seen to be repulsive at short ranges, but changes sign at longer ranges.

4. If one adds an additional pole to such a solution, this pole (or another) will be pushed to infinity along the imaginary axis. If the system has less than $N(L)$ poles it is unstable to the addition of poles, and any noise will drive the system towards this unique state. The number $N(L)$ is

$$N(L) = \left[\frac{1}{2}\left(\frac{L}{\nu} + 1\right)\right], \tag{13}$$

where $\Big[\dots\Big]$ is the integer part. To see this consider a system with N poles and such that all the values of y_j satisfy the condition $0 < y_j < y_{max}$. Add now one additional pole whose coordinates are $z_a \equiv (x_a, y_a)$ with $y_a \gg y_{max}$. From the equation of motion for y_a, (12) we see that the terms in the sum are all of the order of unity as is also the $\cot(y_a)$ term. Thus the equation of motion of y_a is approximately

$$\frac{dy_a}{dt} \approx \nu \frac{2N+1}{L^2} - \frac{1}{L} \ . \tag{14}$$

The fate of this pole depends on the number of other poles. If N is too large the pole will run to infinity, whereas if N is small the pole will be attracted towards the real axis. The condition for moving away to infinity is that $N > N(L)$ where $N(L)$ is given by (13). On the other hand the y coordinate of the poles cannot hit zero. Zero is a repulsive line, and poles are pushed away from zero with infinite velocity. To see this consider a pole whose y_j approaches zero. For any finite L the term $\coth(y_j)$ grows unboundedly whereas all the other terms in Eq.(12) remain bounded.

5. The height of the cusp is proportional to L. The distribution of positions of the poles along the line of constant x was worked out in [15].

We will refer to the solution with all these properties as the Thual-Frisch-Henon (TFH)-cusp solution.

2.2 Nonlinear Stability

The intuition gained so far can be used to discuss the issue of stability of a stable system to *larger* perturbations. In other words, we may want to add to the system poles at finite values of y and ask about their fate. We first show in this subsection that poles whose initial y value is below $y_{max} \sim \log(L^2/\nu^2)$ will be attracted towards the real axis. The scenario is similar to the one described in the last paragraph.

Suppose that we generate a stable system with a giant cusp at $\theta_c = 0$ with poles distributed along the y axis up to y_{max}. We know that the sum of all the forces that act on the upper pole is zero. Consider then an additional pole inserted in the position (π, y_{max}). It is obvious from Eq.(12) that the forces acting on this pole will pull it downward. On the other hand if its initial position is much above y_{max} the force on it will be repulsive towards infinity. We see that this simple argument identifies y_{max} as the typical scale for nonlinear instability.

Next we estimate y_{max} and interpret our result in terms of the *amplitude* of a perturbation of the flame front. We explained that uppermost pole's position fluctuates between a minimal value and infinity as L is changing. We want to estimate the characteristic scale of the minimal value of $y_{max}(L)$. To this aim we employ the result of ref.[15] regarding the stable distribution of pole positions in a stable large system. The parametrization of [15] differs from ours; to go from our parametrization in Eq.(5) to theirs we need to rescale u by L^{-1} and t by L. The parameter ν in their parameterization is ν/L in ours. According to [15] the number of poles between y and $y + dy$ is

given by the $\rho(y)dy$ where the density $\rho(y)$ is

$$\rho(y) = \frac{L}{\pi^2 \nu} \ln[\coth(|y|/4)] \ . \tag{15}$$

To estimate the minimal value of y_{max} we require that the tail of the distribution $\rho(y)$ integrated between this value and infinity will allow one single pole. In other words,

$$\int_{y_{max}}^{\infty} dy \rho(y) \approx 1 \ . \tag{16}$$

Expanding (15) for large y and integrating explicitly the result in (16) we end up with the estimate

$$y_{max} \approx 2 \ln \left[\frac{4L}{\pi^2 \nu} \right] \tag{17}$$

For large L this result is $y_{max} \approx \ln(\frac{L^2}{\nu^2})$. If we now add an additional pole in the position (θ, y_{max}) this is equivalent to perturbing the solution $u(\theta, t)$ with a function $\nu e^{-y_{max}} \sin(\theta)$, as can be seen directly from (8). We thus conclude that the system is unstable to a perturbation *larger* than

$$u(\theta) \sim \nu^3 \sin(\theta)/L^2 \ . \tag{18}$$

This indicates a very strong size dependence of the sensitivity of the giant cusp solution to external perturbations. This will be an important ingredient in our discussion of noisy systems.

3 Acceleration of the Flame Front, Pole Dynamics and Noise

A major motivation of this Section is the observation that in radial geometry the same equation of motion shows an acceleration of the flame front. The aim of this section is to argue that this phenomenon is caused by the noisy generation of new poles. Moreover, it is our contention that a great deal can be learned about the acceleration in radial geometry by considering the effect of noise in channel growth. In Ref. [15] it was shown that any initial condition which is represented in poles goes to a unique stationary state which is the giant cusp which propagates with a constant velocity $v = 1/2$ up to small $1/L$ corrections. In light of our discussion of the last section we expect that any smooth enough initial condition will go to the same stationary state. Thus if there is no noise in the dynamics of a finite channel, no acceleration of the flame front is possible. What happens if we add noise to the system?

For concreteness we introduce an additive white-noise term $\eta(\theta, t)$to the equation of motion (5) where

$$\eta(\theta, t) = \sum_k \eta_k(t) \exp(ik\theta) \ , \tag{19}$$

and the Fourier amplitudes η_k are correlated according to

$$< \eta_k(t) \eta^*_{k'}(t') >= \frac{f}{L} \delta_{k,k'} \delta(t - t') \ . \tag{20}$$

We will first examine the result of numerical simulations of noise-driven dynamics, and later return to the theoretical analysis.

3.1 Noisy Simulations

Previous numerical investigations [5, 23] did not introduce noise in a controlled fashion. We will argue later that some of the phenomena encountered in these simulations can be ascribed to the (uncontrolled) numerical noise. We performed numerical simulations of Eq.(5 using a pseudo-spectral method. The time-stepping scheme was chosen as Adams-Bashforth with 2nd order presicion in time. The additive white noise was generated in Fourier-space by choosing η_k for every k from a flat distribution in the interval $[-\sqrt{2\frac{f}{L}}, \sqrt{2\frac{f}{L}}]$. We examined the average steady state velocity of the front as a function of L for fixed f and as a function of f for fixed L. We found the interesting phenomena that are summarized here:

1. In Fig.1 we can see two different regimes of behavior the average velocity v as function of noise $f^{0.5}$ for fixed system size L. For the noise f smaller then same fixed value f_{cr}
$$v \sim f^{\xi} \ . \tag{21}$$
For these values of f this dependence is very weak, and $\xi \approx 0.02$. For large values of f the dependence is much stronger

2. In Fig.2 we can see growth of the average velocity v as function of the system size L. After some values of L we can see saturation of the velocity. For regime $f < f_{cr}$ the growth of the velocity can be written as
$$v \sim L^{\mu}, \quad \mu \approx 0.40 \pm 0.05 \ . \tag{22}$$

3.2 Calculation of Poles Number in the System

The interesting problem that we would like to solve here it is to find number of poles that exist in our system outside the giant cusp. We can make it by next way: to calculate number of cusps (points of minimum or inflexional points) and their position on the interval $\theta : [0, 2\pi]$ in every moment of time and to draw positions of cusp like function of time, see Fig.3.

We assume that our system is almost all time in "quasi-stable" state, i.e. every new cusp that appears in the system includes only one pole. By help pictures obtained by such way we can find

1. By calculation number of cusp in some moment of time and by investigation of history of every cusp (except the giant cusp) , i.e. how many initial cusps take part in formation this cusp, after averaging with respect to different moments of time we can find mean number of poles that exist in our system outside the giant cusp. Let us denote this number δN. We can see four regimes that can be define with respect to dependence of this number on noise f:

(i) Regime I: Such small noise that no poles exist in our system outside the giant cusp.

(ii) Regime II Strong dependence of poles number δN on noise f.

(iii) Regime III Saturation poles number δN on noise f, so we see very small dependence of this number on noise

$$\delta N \sim f^{0.03} \tag{23}$$

Saturated value of δN is defined by next formula

$$\delta N \approx N(L)/2 \approx \frac{1}{4}\frac{L}{\nu} \tag{24}$$

where $N(L) \approx \frac{1}{2}\frac{L}{\nu}$ is number of poles in giant cusp.

(iv) Regime IV We again see strong dependence of poles number δN on noise f.

$$\delta N \sim f^{0.1} \tag{25}$$

Because of numerical noise we can see in most of simulations only regime III and IV. In future if we don't note something different we discuss regime III.

2. By calculation of new cusp number we can find number of poles that appear in the system in unit of time $\frac{dN}{dt}$. In regime III

$$\frac{dN}{dt} \sim f^{0.03} \tag{26}$$

Dependence on L and ν define by

$$\frac{dN}{dt} \sim L^{0.8} \tag{27}$$

$$\frac{dN}{dt} \sim \frac{1}{\nu^2} \tag{28}$$

And in regime IV

$$\frac{dN}{dt} \sim f^{0.1} \tag{29}$$

3.3 Theoretical Discussion of the Effect of Noise

3.3.1 The Threshold of Instability to Added Noise. Transition from regime I to regime II

First we present the theoretical arguments that explain the sensitivity of the giant cusp solution to the effect of added noise. This sensitivity increases dramatically with increasing the system size L. To see this we use again the relationship between the linear stability analysis and the pole dynamics.

Our additive noise introduces perturbations with all k-vectors. We showed previously that the most unstable mode is the $k = 1$ component $A_1 \sin(\theta)$. Thus the most effective noisy perturbation is $\eta_1 \sin(\theta)$ which can potentially lead to a growth of the most unstable mode. Whether or not this mode will grow depends on the amplitude of the noise. To see this clearly we return to the pole description. For small values of the amplitude A_1 we represent $A_1 \sin(\theta)$ as a single pole solution of the functional form $\nu e^{-y} \sin\theta$. The y position is determined from $y = -\log|A_1|/\nu$, and the θ-position is $\theta = \pi$ for positive A_1 and $\theta = 0$ for negative A_1. For very small A_1 the fate of the pole is to be pushed to infinity, independently of its θ position; the dynamics is symmetric in $A_1 \to -A_1$ when y is large enough. On the other hand when the value of A_1 increases the symmetry is broken and the θ position and the sign of A_1 become very important. If $A_1 > 0$ there is a threshold value of y below which the pole is attracted down. On the other hand if $A_1 < 0$, and $\theta = 0$ the repulsion from the poles of the giant cusp grows with decreasing y. We thus understand that qualitatively speaking the dynamics of A_1 is characterized by an asymmetric "potential" according to

$$\dot{A}_1 = -\frac{\partial V(A_1)}{\partial A_1} , \tag{30}$$

$$V(A_1) = \lambda A_1^2 - a A_1^3 + \dots . \tag{31}$$

From the linear stability analysis we know that $\lambda \approx \nu/L^2$, cf. Eq.(14). We know further that the threshold for nonlinear instability is at $A_1 \approx \nu^3/L^2$, cf. Eq(18). This determines that value of the coefficient $a \approx 2/3\nu^2$. The magnitude of the "potential" at the maximum is

$$V(A_{max}) \approx \nu^7/L^6 . \tag{32}$$

The effect of the noise on the development of the mode $A_1 \sin\theta$ can be understood from the following stochastic equation

$$\dot{A}_1 = -\frac{\partial V(A_1)}{\partial A_1} + \eta_1(t) . \tag{33}$$

It is well known [24] that for such dynamics the rate of escape R over the "potential" barrier for small noise is proportional to

$$R \sim \frac{\nu}{L^2} \exp^{-\nu^7/\frac{f}{L}L^6} . \tag{34}$$

The conclusion is that any arbitrarily tiny noise becomes effective when the system size increase and when ν decreases. If we drive the system with noise of amplitude $\frac{f}{L}$

the system can always be sensitive to this noise when its size exceeds a critical value L_c that is determined by $\frac{f}{L_c} \sim \nu^7/L_c^6$. This formula defines transition from regime I (no poles) to regime II. For $L > L_c$ the noise will introduce new poles into the system. Even numerical noise in simulations involving large size systems may have a macroscopic influence.

The appearance of new poles must increase the velocity of the front. The velocity is proportional to the mean of $(u/L)^2$. New poles distort the giant cusp by additional smaller cusps on the wings of the giant cusp, increasing u^2. Upon increasing the noise amplitude more and more smaller cusps appear in the front, and inevitably the velocity increases. This phenomenon is discussed quantitatively in Section 3.

3.3.2 Verifying of asymmetric "potential" form

From the equations of the motion for poles we can find the distribution of poles in the giant cusp [15]. If we know the distribution of poles in the giant cusp we can then find the form of the "potential" and verify numerically expressions for values λ, A_{max} and $\frac{\partial V(A_1)}{\partial A_1}$ discussed previously. The connection between amplitude A_1 and the position of the pole y is defined by $A_1 = 4\nu e^{-y}$ and the connection between the potential function $\frac{\partial V(A_1)}{\partial A_1}$ and the position of the pole y is defined by formula $\frac{\partial V(A_1)}{\partial A_1} = 4\nu \frac{dy}{dt} e^{-y}$, where $\frac{dy}{dt}$ can be determined from the equation of the motion of the poles. We can find A_{max} as the zero-point of $\frac{\partial V(A_1)}{\partial A_1}$ and λ can be found as $\frac{1}{2}\frac{\partial^2 V(A_1)}{\partial A_1^2}$ for $A_1 = 0$. Numerical measurements were made for the set of values $L = 2n\nu$, where n is a integer and $n > 2$. For our numerical measurements we use the constant $\nu = 0.005$ and the variable L, where L changes in the interval [1,150], or variable ν that changes in the interval [0.005,0.05] and the constant $L = 1$. The results obtained follow:

1. Formula for $\frac{A_{max}L^2}{\nu^3}$

$$\frac{A_{max}L^2}{\nu^3} \approx 6.5 \; . \tag{35}$$

2. Formula for $\frac{A_{max}}{A_{N(L)}}$

$$\frac{A_{max}}{A_{N(L)}} \approx 0.465 \; . \tag{36}$$

   where $A_{N(L)}$ is defined by position of the upper pole.

3. Formula for $\frac{\lambda L^2}{\nu}$

$$\frac{\lambda L^2}{\nu} = 0.5 \; . \tag{37}$$

4. We also verify the boundary between regime I (no new cusps) and regime II (new cusps appear). Fig. 4 shows the dependence of $\frac{f}{L_c}$ on L_c. We can see that $f/L_c \sim 1/L_c^6$.

These results are in good agreement with the theory.

3.3.3 The Noisy Steady State and its Collapse with Large Noise and System Size

In this subsection we discuss the response of the giant cusp solution to noise levels that are able to introduce a large number of excess poles in addition to those existing in the giant cusp. We will denote the excess number of poles by δN. The first question that we address is how difficult is it to insert yet an additional pole when there is already a given excess δN. To this aim we estimate the effective potential $V_{\delta N}(A_1)$ which is similar to (31) but is taking into account the existence of an excess number of poles. A basic approximation that we employ is that the fundamental form of the giant cusp solution is not seriously modified by the existence of an excess number of poles. Of course this approximation breaks down quantitatively already with one excess pole. Qualitatively however it holds well until the excess number of poles is of the order of the original number $N(L)$ of the giant cusp solution. Another approximation is that the rest of the linear modes play no role in this case. At this point we limit the discussion therefore to the situation $\delta N \ll N(L)$ (regime II).

To estimate the parameter λ in the effective potential we consider the dynamics of one pole whose y position y_a is far above y_{max}. According to Eq.(14) the dynamics reads

$$\frac{dy_a}{dt} \approx \frac{2\nu(N(L)+\delta N)}{L^2} - \frac{1}{L} \tag{38}$$

Since the $N(L)$ term cancels against the L^{-1} term (cf. Sec. 2.1), we remain with a repulsive term that in the effective potential translates to

$$\lambda = \frac{\nu \delta N}{L^2} \ . \tag{39}$$

Next we estimate the value of the potential at the break-even point between attraction and repulsion. In the last subsection we saw that a foreign pole has to be inserted below y_{max} in order to be attracted towards the real axis. Now we need to push the new pole below the position of the existing pole whose index is $N(L) - \delta N$. This position is estimated as in Sec 2.2 by employing the TFH distribution function (15). We find

$$y_{\delta N} \approx 2 \ln \left[\frac{4L}{\pi^2 \nu \delta N} \right] \ . \tag{40}$$

As before, this implies a threshold value of the amplitude of single pole solution $A_{max} \sin\theta$ which is obtained from equating $A_{max} = \nu e^{-y_{\delta N}}$. We thus find in the present case $A_{max} \sim \nu^3 (\delta N)^2 / L^2$. Using again a cubic representation for the effective potential we find $a = 2/(3\nu^2 \delta N)$ and

$$V(A_{max}) = \frac{1}{3} \frac{\nu^7 (\delta N)^5}{L^6} \ . \tag{41}$$

Repeating the calculation of the escape rate over the potential barrier we find in the present case

$$R \sim \frac{\nu \delta N}{L^2} \exp^{-\nu^7 (\delta N)^5 / \frac{f}{L} L^6} \ . \tag{42}$$

For a given noise amplitude $\frac{f}{L}$ there is always a value of L and ν for which the escape rate is of $O(1)$ as long as δN is not too large. When δN increases the escape

rate decreases, and eventually no additional poles can creep into the system. The typical number δN for fixed values of the parameters is estimated from equating the argument in the exponent to unity:

$$\delta N \approx \left(\frac{f}{L} L^6/\nu^7\right)^{1/5} . \tag{43}$$

We can see that δN depend on noise f very seriously. It is not the case in regime III. Let us find conditions of transition from regime II to regime III, where we see saturation of δN with respect to noise f.

(i) We use for the amplitude of pole solution that really equal to $\frac{2\nu \sin\theta}{\cosh(y_{\delta N})-\cos\theta}$ expression $A_{max} = 4\nu e^{-y_{\delta N}}$ but it is right only for big number $y_{\delta N}$. For $y_{\delta N} < 1$ better approximation is $A_{max} = \frac{4\nu}{y_{\delta N}^2}$. From equation (40) we can find that the boundary value $y_{\delta N} = 1$ correspond to $\delta N \approx N(L)/2$

(ii) We use expression $y_{\delta N} \approx 2\ln\left[\frac{4L}{\pi^2\nu\delta N}\right]$ but for big value of δN better approximation that can be find the same way is $y_{\delta N} \approx \frac{\pi^2\nu}{2L}(N(L)-\delta N)\ln\left[\frac{8eL}{\pi^2\nu(N(L)-\delta N)}\right]$. These expressions give us nearly equal result for $\delta N \approx N(L)/2$.

From (i) and (ii) we can make next conclusions

(a) Transition from regime II to regime III happens for nearly $\delta N \approx N(L)/2$

(b) Using new expression in (i) and (ii) for amplitude A_{max} and $y_{\delta N}$ we can find for noise $\frac{f}{L}$ in regime III:

$$\frac{f}{L} \sim V(A_{max}) \sim \lambda A_{max}^2 \sim \frac{\nu\delta N}{L^2}(\frac{4\nu}{y_{\delta N}^2})^2 \sim \frac{L^2}{\nu}\frac{\delta N}{(N(L)-\delta N)^4} \tag{44}$$

This expression define very slow dependence of δN on noise $\frac{f}{L}$ for $\delta N > N(L)/2$ that explain noise saturation of δN for regime III.

(c) Form of the giant cusp solution is defined by poles that are closely to zero with respect to y. For regime III $N(L)/2$ poles that have position $y < y_{\delta N = N(L)/2} = 1$ stay on these place. This result explain why giant cusp solution is not seriously modified for regime III.

From Eq.(43) by help of boundary condition

$$\delta N \approx N(L)/2 \tag{45}$$

boundary noise f_b between regime II and III can be found

$$f_b \sim \nu^2 \tag{46}$$

The basic equation describing pole dynamics is next

$$\frac{dN}{dt} = \frac{\delta N}{T} \tag{47}$$

where $\frac{dN}{dt}$ is number of poles that appear in unit of time in our system, δN is excess number of poles, T is mean life time of pole (between appearing and merging with giant cusp). Using result of numerical simulations for $\frac{dN}{dt}$ and (45) we can find for T

$$T = \frac{\delta N}{\frac{dN}{dt}} \sim \nu L^{0.2} \tag{48}$$

So life time proportional to ν and depend on system size L very weakly.

Moreover, the lifetime of a pole is defined by the lifetime of the poles that are in a cusp. From the maximum point of the linear part of Eq.(1), we can find the mean character size

$$\lambda_m \sim \nu \tag{49}$$

that defines the size of our cusps. This result was confirmed in numerical calculations executed in [25]. Indeed, we can see it from Fig.9 in [25]. The mean number of poles in a cusp

$$n_{big} \approx \frac{\lambda_m}{2\nu} \sim const \tag{50}$$

does not depend on L and ν. The mean number of cusps is

$$N_{big} \sim \frac{\delta N}{n_{big}} \sim \frac{L}{\nu} \, . \tag{51}$$

Let us assume that some cusp exists in the main minimum of the system. The lifetime of a pole in such a cusp is defined by three parts.

(I) Time of the cusp formation. This time is proportional to the cusp size (with $\ln$-corrections) and the pole number in the cusp (from pole motion equations)

$$T_1 \sim \lambda_m n_{big} \sim \nu \tag{52}$$

(II) Time that the cusp is in the minimum neighborhood. This time is defined by

$$T_2 \sim \frac{a}{v} \tag{53}$$

where a is a neighborhood of minimum, such that the force from the giant cusp is smaller than the force from the fluctuations of the excess pole number δN, and v is the velocity of a pole in this neighborhood. Fluctuations of excess pole number δN are expressed as

$$N_{fl} = \sqrt{\delta N} \, . \tag{54}$$

From this result and the pole motion equations we find that

$$v \sim \frac{\nu}{L} N_{fl} \sim \frac{\nu}{L} \sqrt{\frac{L}{\nu}} \sim \sqrt{\frac{\nu}{L}} \, . \tag{55}$$

The velocity from the giant cusp is defined by

$$v \sim \frac{\nu}{L} N(L) \frac{a}{L} \sim \frac{a}{L} \, . \tag{56}$$

So from equating these two equations we obtain

$$a \sim \sqrt{\nu L} \; . \tag{57}$$

Thus for T_2 we obtain

$$T_2 \sim \frac{a}{v} \sim L \; . \tag{58}$$

(III) Time of attraction to the giant cusp. From the equations of motion for the poles we get

$$T_3 \sim L \ln(\frac{L}{a}) \sim L \ln \sqrt{L} \sim L \; . \tag{59}$$

The investigated domain of the system size was found to be

$$T_1 \gg T_2, T_3 \tag{60}$$

Therefore full lifetime is

$$T = T_1 + T_2 + T_3 \sim \nu + sL \; , \tag{61}$$

where s is a constant and

$$0 < s \ll 1 \; . \tag{62}$$

This result qualitatively and partly quantatively explains dependence (48). From (48), (47), (45) we can see that in regime III $\frac{dN}{dt}$ is saturated with the system size L.

3.4 The acceleration of the flame front due to noise

In this section we estimate the scaling exponents that characterize the velocity of the flame front as a function of the system size. Our arguments in this section are even less solid than the previous ones, but nevertheless we believe that we succeed to capture some of the essential qualitative physics that underlies the interaction between noise and instability and which results in the acceleration of the flame front.

To estimate the velocity of the flame front we need to write down an equation for the mean of $< dh/dt >$ given an arbitrary number N of poles in the system. This equation follows directly from (4):

$$\left\langle \frac{dh}{dt} \right\rangle = \frac{1}{L^2} \frac{1}{2\pi} \int_0^{2\pi} u^2 d\theta \; . \tag{63}$$

After substitution of (8) in (63) we get, using (11) and (12)

$$\left\langle \frac{dh}{dt} \right\rangle = 2\nu \sum_{k=1}^{N} \frac{dy_k}{dt} + 2 \left(\frac{\nu N}{L} - \frac{\nu^2 N^2}{L^2} \right) \; . \tag{64}$$

The estimates of the second and third terms in this equation are straightforward. Writing $N = N(L) + \delta N(L)$ and remembering that $N(L) \sim L/\nu$ and $\delta N(L) \sim N(L)/2$ we find that these terms contribute $O(1)$. The first term will contribute only when

the current of poles is asymmetric. Since noise introduces poles at a finite value of y_{min}, whereas the rejected poles stream towards infinity and disappear at boundary of nonlinearity defined by position of highest pole

$$y_{max} \approx 2 \ln \left[\frac{4L}{\pi^2 \nu} \right] . \tag{65}$$

, we have an asymmetry that contributes to the velocity of the front. To estimate the first term let us define

$$d(\sum \frac{dy_k}{dt}) = \sum_{l}^{l+dl} \frac{dy_k}{dt} \tag{66}$$

where $\sum_{l}^{l+dl} \frac{dy_k}{dt}$ is sum over poles that are on the interval $y : [l, l + dl]$. We can write

$$d(\sum \frac{dy_k}{dt}) = d(\sum \frac{dy_k}{dt})_{up} - d(\sum \frac{dy_k}{dt})_{down} \tag{67}$$

Where $d(\sum \frac{dy_k}{dt})_{up}$ flux of poles moving up and $d(\sum \frac{dy_k}{dt})_{down}$ flux of poles moving down.

For these flux we can write

$$d(\sum \frac{dy_k}{dt})_{up}, d(\sum \frac{dy_k}{dt})_{down} \leq \frac{dN}{dt} dl \tag{68}$$

So for the first term

$$\begin{aligned} & 0 \leq \sum_{k=1}^{N} \frac{dy_k}{dt} = \\ & \int_{y_{min}}^{y_{max}} \frac{d(\sum \frac{dy_k}{dt})}{dl} dl \\ & = \int_{y_{min}}^{y_{max}} \frac{d(\sum \frac{dy_k}{dt})_{up} - d(\sum \frac{dy_k}{dt})_{down}}{dl} dl \\ & \leq \frac{dN}{dt} (y_{max} - y_{min}) \\ & \leq \frac{dN}{dt} y_{max} \end{aligned} \tag{69}$$

Because of slow($\ln$) dependence of y_{max} on L and ν $\frac{dN}{dt}$ term define oder of nonlinearity for first term. This term zero for symmetric current of poles and achieves maximum for maximal asymmetric current of poles. Comparison $v \sim L^{0.42} f^{0.02}$ and $\frac{dN}{dt} \sim L^{0.8} f^{0.03}$ confirm this calculation.

4 summary and conclusions

The main two messages of this paper like the previous one are: (i) There is an important interaction between the instability of developing fronts and random noise; (ii) This interaction and its implications can be understood qualitatively and sometimes quantitatively using the description in terms of complex poles.

The pole description is natural in this context firstly because it provides an exact (and effective) representation of the steady state without noise. Once one succeeds to describe also the *perturbations* about this steady state in terms of poles, one achieves a particularly transparent language for the study of the interplay between noise and instability. This language also allows us to describe in qualitative and semi-quantitative terms the inverse cascade process of increasing typical lengths when the system relaxes to the steady state from small, random initial conditions.

The main conceptual steps in this paper are as follows: firstly one realizes that the steady state solution, which is characterized by $N(L)$ poles aligned along the imaginary axis is marginally stable against noise in a periodic array of L values. For all values of L the steady state is nonlinearly unstable against noise. The main and foremost effect of noise of a given amplitude f is to introduce an excess number of poles $\delta N(L, f)$ into the system. The existence of this excess number of poles is responsible for the additional wrinkling of the flame front on top of the giant cusp, and for the observed acceleration of the flame front. By considering the noisy appearance of new poles we rationalize the observed scaling laws as a function of the noise amplitude and the system size.

The "phase diagram" as a function of L and f in this system consists of four regimes (in contradiction with our previous results [6]). In the first one, discussed in Section 3.3.1 , the noise is too small to have any effect on the giant cusp solution. The second regime (very small excess number of poles) can not be observed because of numerical noise and discussed only theoretically. In the third regime the noise introduces excess poles that serve to decorate the giant cusp with side cusps. In this regime we find scaling laws for the velocity as a function of L and f and we are reasonably successful in understanding the scaling exponents. In the fourth regime the noise is large enough to create small scale structures that are not neatly understood in terms of individual poles. It appears from our numerics that in this regime the roughening of the flame front gains a contribution from the the small scale structure in a way that is reminiscent of *stable*, noise driven growth models like the Kardar-Parisi-Zhang model.

One of our main motivations in this research was to understand the phenomena observed in radial geometry with expanding flame fronts. A full analysis of this problem cannot be presented here. We note however that many of the insights offered above translate immediately to that problem. Indeed, in radial geometry the flame front accelerates and cusps multiply and form a hierarchic structure as time progresses. Since the radius (and the typical scale) increase in this system all the time, new poles will be added to the system even by a vanishingly small noise. The marginal stability found above holds also in this case, and the system will allow the introduction of excess poles as a result of noise. The results discussed in Ref.[7] can be combined with the present insights to provide a theory of radial growth. This theory was offered in Ref.[8].

We have had a serious open problem for this case [10], but this problem was solved

successfully recently Karlin and Sivashinsky [12] , [13]. For a cylindrical case of the flame front propagation problem at absence of noise (only numerical noise Ref.[26, 27, 28, 29, 30]) by Sivashinsky with help of numerical methods it was shown, that the flame front is continuously accelerated. During all this account time it is not visible any attributes of saturation. To increase time of the account is a difficult task. Hence, absence or presence of velocity saturation in a cylindrical case, as consequence of the flame front motion equation it was a open problem before appearance of the papers [12] , [13].

For the best understanding of dependence of flame front velocity as functions of its radius in a cylindrical case similar dependence of flame front velocity on width of the channel (in a flat case) also was analyzed by numerical methods. Growth of velocity is also observed and at absence of noise (only numerical noise!) also any saturation of the velocity it is not observed. Introduction obvious Gaussian noise results to appearance of a point of saturation and its removal from the origin of coordinates with decreasing of noise amplitude, allowing extrapolating results on small numerical noise. (Fig.2)

Hence, introducing of Gaussian noise in numerical calculation also for a cylindrical case can again results to appearance of a saturation point and will allow to investigate its behavior as function of noise amplitude by extrapolating results on small numerical noise. This investigation was really made and saturation was observed recently by Karlin and Sivashinsky [12] , [13] for 1D, 2D and 3D cases.

Finally, the success of this approach in the case of flame propagation demonstrates that Laplacian growth patterns can be dealt with using similar ideas. A problem of immediate interest is Laplacian growth in channels, in which a finger steady-state solution is known to exist. It is documented that the stability of such a finger solution to noise decreases rapidly with increasing the channel width. In addition, it is understood that noise brings about additional geometric features on top of the finger. There are enough similarities here to indicate that a careful analysis of the analytic theory may shed as much light on that problem as on the present one.

Acknowledgments The authors are grateful to the anonymous referee for various suggestions to improve the clarity of the paper. We would like also to thank Itamar Procaccia for his supervision and many fruitful ideas result in creating the paper. We also would like to thank Barak Galanti for all necessary numerical calculations executed for this paper.

References

[1] Liberman M.A., Ivanov M.F., Peil O.E., Valiev D.M., Eriksson L.-E. Self-acceleration and fractal structure of outward freely propagating flames // Physics of Fluids. - 2004. - V. 16, N 7. - PP. 2476-2482

[2] Gostintsev Yu.A., Istratov A.G., Shulenin Yu.V. Self-similar propagation of a free turbulent flame in mixed gas mixtures // Combust. Expl. Shock Waves. - 1988.- V. 24, N 5. - PP. 63-70

[3] Wu F., Jomaas G., Law C.K. On Self-Acceleration of Cellular Spherical Flames // Fall Technical Meeting of the Eastern States Section of the Combustion Institute Hosted by the University of Connecticut, Storrs, CT - 2011. - http://lcg.princeton.edu/publications/conference-publications/wu-on-self-acceleration-of-cellular-spherical-flames.

[4] Sivashinsky G.I. Nonlinear analysis of hydrodynamics instability in laminar ames I. Deriva- tions fo basic equations Nonlinear analysis of hydrodynamics instability in laminar ames I. Deriva- tions fo basic equations // Acta Astronautica - 1977. - V. 4 - PP. 1177-1206

[5] Filyand L., Sivashinsky G.I., Frankel M.L. On self-acceleration of outward propagating wrinkled flames // Physica D - 1994. - V. 72 - PP. 110-118

[6] Olami Z., Glanti B., Kupervasser O., Procacccia I. Random Noise and Pole-Dynamics in Unstable Front Propagation // Phys. Rev. E. - 1997. - V. 55, N 3 - PP. 2649-2663

[7] Kupervasser O., Olami Z., Procacccia I. Geometry of Developing Flame Fronts: Analysis with Pole Decomposition // Phys. Rev. Lett. - 1996. - V. 76 - PP. 146-149

[8] B. Glanti, Kupervasser O., Olami Z., Procacccia I. Dynamics and Wrinkling of Radially Propagation Fronts Inferred from Scaling Law in Channel Geometries // Phys. Rev. Lett. - 1998. - V. 80, N 11 - PP. 2477-2480

[9] Kupervasser O., Olami Z., Procacccia I. Stability Analysis of Flame Fronts: Dynamical Systems Approach in the Complex Plane // Phys. Rev. E - 1999. - V. 59, N 3 - PP. 2587-2593

[10] Kupervasser O. Pole solutions in the case of problems of flame front propagation and Saffman-Teylor ”finger” formation without surface tension: open problems and possible ways of their solutions - 2003. - arXiv:nlin/0306038

[11] Kupervasser O. Random Noise and Pole-Dynamics in Unstable Front Propagation - 2003. - arXiv:nlin/0302017

[12] Karlin V., Sivashinsky G. The Rate of Expansion of Spherical Flames // Combustion Theory and Modelling - 2006. - V. 10, N 4 - PP. 625-637

[13] Karlin V., Sivashinsky G. Asymptotic modelling of self-acceleration of spherical flames // Proceedings of the Combustion Institute - 2007. - V. 31, N 1 - PP. 1023-1030

[14] Lee Y.C., Chen H.H. Nonlinear dynamical models of plasma turbulence // Phys. Scr. (Sweden) - 1982.- T2A - PP. 41-47

[15] O. Thual, U.Frisch and M. Henon Application of pole decomposition to an equation governing the dynamics of wrinkled flame fronts // J. Physique - 1985. - V. 46, PP. 1485-1494

[16] Joulin G. On the hydrodynamic stability of curved premixed flames // J. Phys. France - 1989. - V. 50 - PP. 10691082

[17] Joulin G. On the Zhdanov-Trubnikov equation for premixed flame instability // J. Exp.Theor. Phys. -1990.-V. 100, Is.2(8) - PP. 428-432

[18] Minaev S.S. Set of steady solutions describing a cellular flame in the case of hydrodynamic instability // Combustion, Explosion, and Shock Waves - 1992. - V. 28, N 1 - PP. 3539

[19] Minaev S.S., Pirogov E.A., Sharypov O.V. A Nonlinear model of hydrodynamic instability of outward propagating flame // Combustion, Explosion, and Shock Waves - 1996. - V. 32, N 5 - PP. 481-488

[20] Fursenko R.V., Pan K.L., Minaev S.S. Noise influence on pole solutions of the Sivashinsky equation for planar and outward propagating flames // PHYS. REV.E - 2008. - V. 78, N 5 - P. 056301

[21] Pan K.L., Fursenko R.V. Characteristics of cylindrical flame acceleration in outward expansion // PHYSICS OF FLUIDS - 2008. - V. 20, N 9 - P. 094107

[22] Fursenko R.V., Minaev S.S., Pan K.L. Hydrodynamic Instability of Inward-Propagating Flames // Combustion, Explosion, and Shock Waves - 2009. - V. 45, N 5, PP. 511-517

[23] Gutman S., Sivashinsky G.I. The cellular nature of hydrodynamic instability// Physica D - 1990. - V. 43 PP. 129-139

[24] Risken H. The Fokker -Planck Equation. - Berlin: Springer, 1984 (P.124 Eq.(5.111))

[25] Cambray P., Joulin G. Length-Scales of Wrinkling of Weakly-Forced, Unstable Premixed Flames // Combust. Sci. Tech. - 1994. - V. 97 PP. 405428

[26] Rahibe M., Aubry N., Sivashinsky G.I., Lima R. Formation of wrinkles in outwardly propagating flames // Phys. Rev. E - 1995. - V. 52, N 4 - PP. 36753686

[27] Rahibe M., Aubry N., Sivashinsky G.I. Stability of pole solution for planar propagating flames // Phys. Rev. E - 1996. - V. 54, N 5 - PP. 4958-4972

[28] Rahibe M., Aubry N., Sivashinsky G.I. Instability of pole solutions for planar propagating flames in sufficiently large domains // Combust. Theory Modelling - 1998. - V. 2, N 1 - PP. 19 41

[29] Ashurst Wm.T. Darrieus-Landau instability, growing cycloids and expanding flame acceleration // Combust. Theory Modelling - 1997. - V. 1 - PP. 405428

[30] Kortsarts Y., Brailovsky I., Sivashinsky G.I. On Hydrodynamic Instability of Stretched Flames // Combust. Sci. Tech. - 1997. - V. 123 - PP. 207225

Figures Legends

Fig.1: The dependence of the average velocity v on the noise $f^{0.5}$ for L=10, 40, 80.

Fig.2: The dependence of the average velocity v on the system size L for $f^{0.5} = 0, 2.7*10^{-6}, 2.7*10^{-5}, 2.7*10^{-4}, 2.7*10^{-3}, 2.7*10^{-2}, 2.7*10^{-1}$, 0.5, 1.3, 2.7 .

Fig.3: The dependence of the cusps positions on time.$L = 80$ $\nu = 0.1$ $f = 9*10{-}6$

Fig.4: The first odd eigenfunction obtained from traditional stability analysis.

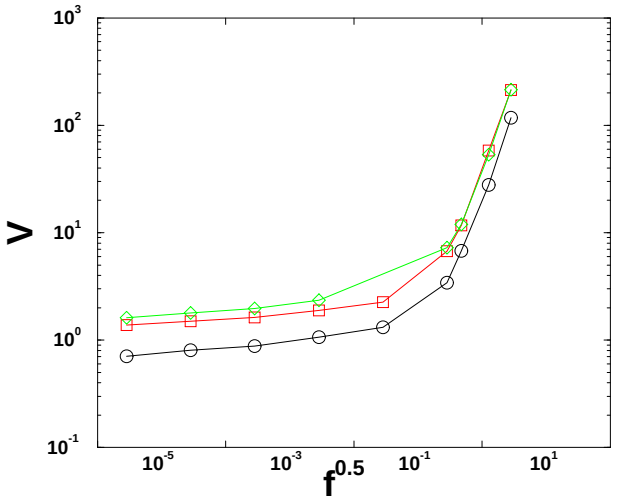

Figure 1:

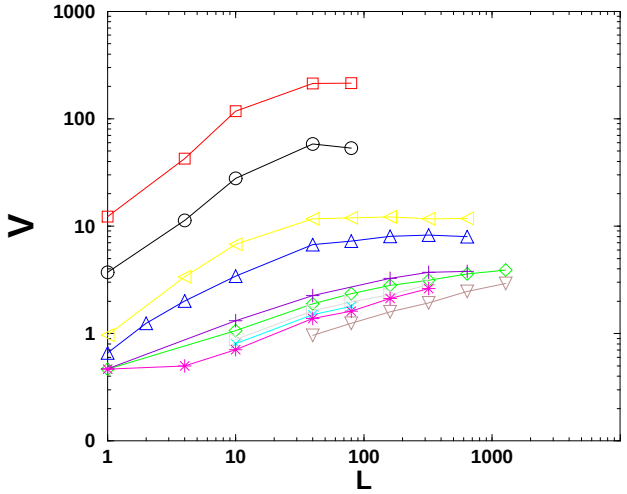

Figure 2:

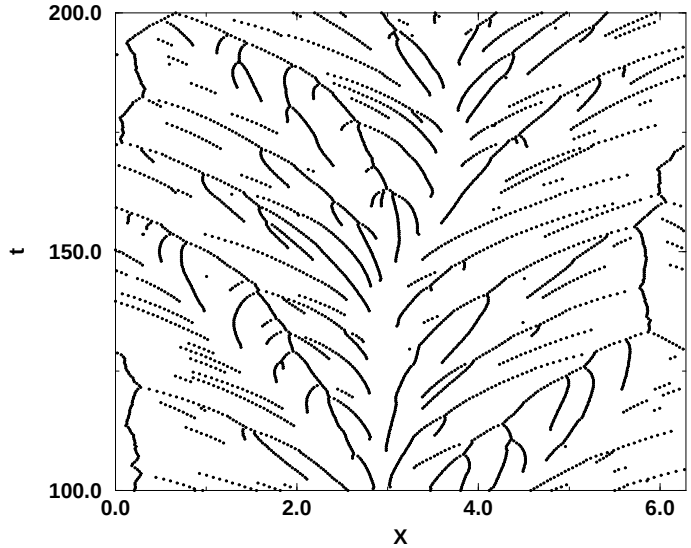

Figure 3:

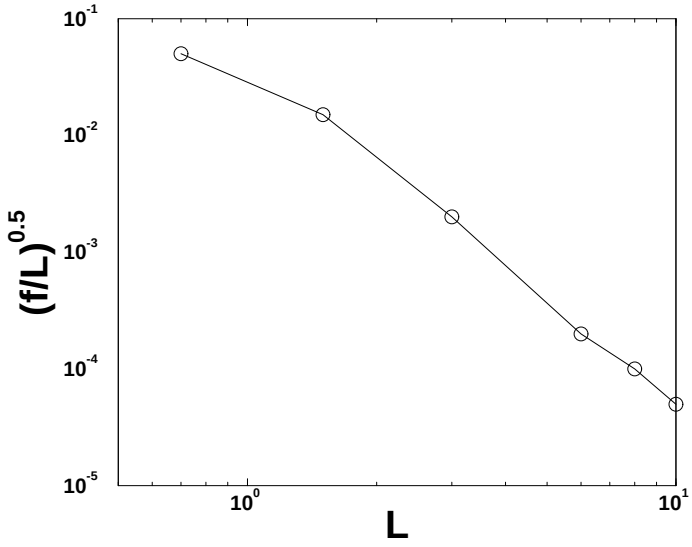

Figure 4: